nature communications

Article

https://doi.org/10.1038/s41467-026-75790-3

Synnovation and confluence explain disparities in species richness across the Andes and Hengduan-Himalaya Mountains

Received: 27 February 2026

Accepted: 8 July 2026

Published online: 23 July 2026

Check for updates

Chih-Chieh Yu[1,2], Zhi-Qiang Du[1], Renske E. Onstein[3,4], Shu-Feng Li[1,5], Richard H. Ree[2,6] ✉ & Yao-Wu Xing[1,5,6] ✉

Mountain regions harbor extraordinary biodiversity, yet the mechanisms underlying this pattern remain unclear. Here we use the phylogenetically and geographically replicated radiations of *Berberis* (barberries) in the Andes and Hengduan–Himalaya Mountains (HHM) to test how functional trait innovations, orogeny, and climate change influenced the buildup of species richness in each region. In barberries (*Berberis*), the successive evolution of deciduousness and small, densely-veined leaves enabled the lineage to take advantage of expanding alpine and subalpine habitats in the HHM during the Miocene. The resulting pulse in the origin of new species contrasts with the more modest rate of species accumulation in the Andes, where barberry species remained evergreen and the availability of high-elevation habitats was more limited. In this study, the phylogeny of barberries exemplifies context-dependent macroevolutionary dynamics, in which intrinsic innovations and extrinsic ecological opportunities interacted to generate exceptional plant diversity in a mountain hotspot.

A conspicuous pattern in global biodiversity is the concentration of species in mountains[1,2]. In plants, a growing body of research has demonstrated that in situ lineage diversification is an important contributor to the assembly of mountain floras[3,4], and that the tempo of this process can be influenced by a variety of abiotic and biotic factors, such as orogeny, climate change[5,6], and the evolution of functional traits[7,8]. Understanding the ways in which these factors may interact synergistically to drive rates of species diversification is an important challenge in biogeography[9–11]. In this context, comparative analysis of phylogenetically and/or geographically replicated instances of in situ diversification can provide more power to distinguish meaningful effects from confounding factors, compared to studies of single clades in single regions[12,13].

A study system that offers the potential for both phylogenetic and geographic replication is found in *Berberis* (Berberidaceae), a lineage of flowering plants with centers of diversity in the Andes (~109 spp.) and the Hengduan-Himalaya Mountains (~247 spp., HHM; excluding the Qinghai–Tibet Plateau; Fig. 1). This pattern presents an opportunity to study a natural experiment in which regional pools of closely related species have evolved independently in widely separated mountain ranges. What biotic and abiotic factors promoted diversification of *Berberis* in these regions? Are these factors shared or region-specific? Why are there more species in the HHM compared to the Andes?

An appropriate null hypothesis for such questions is that rates of diversification do not vary significantly across regions, time, or clades[14,15]; the higher richness of the HHM is due simply to greater time

[1]Applied Research Center for Tropical Plant Conservation, Xishuangbanna Tropical Botanical Garden, Chinese Academy of Sciences, Mengla, Yunnan, China. [2]Department of Collections, Conservation, and Research, Field Museum, Chicago, Illinois, USA. [3]Naturalis Biodiversity Center, Leiden, The Netherlands. [4]Institute of Biology Leiden (IBL), Leiden University, Leiden, The Netherlands. [5]State Key Laboratory of Plant Diversity and Specialty Crops, Xishuangbanna Tropical Botanical Garden, Chinese Academy of Sciences, Mengla, Yunnan, China. [6]These authors jointly supervised this work: Richard H. Ree, Yao-Wu, Xing. ✉e-mail: rree@fieldmuseum.org; ywxing@xtbg.org.cn

https://doi.org/10.1038/s41467-026-75790-3

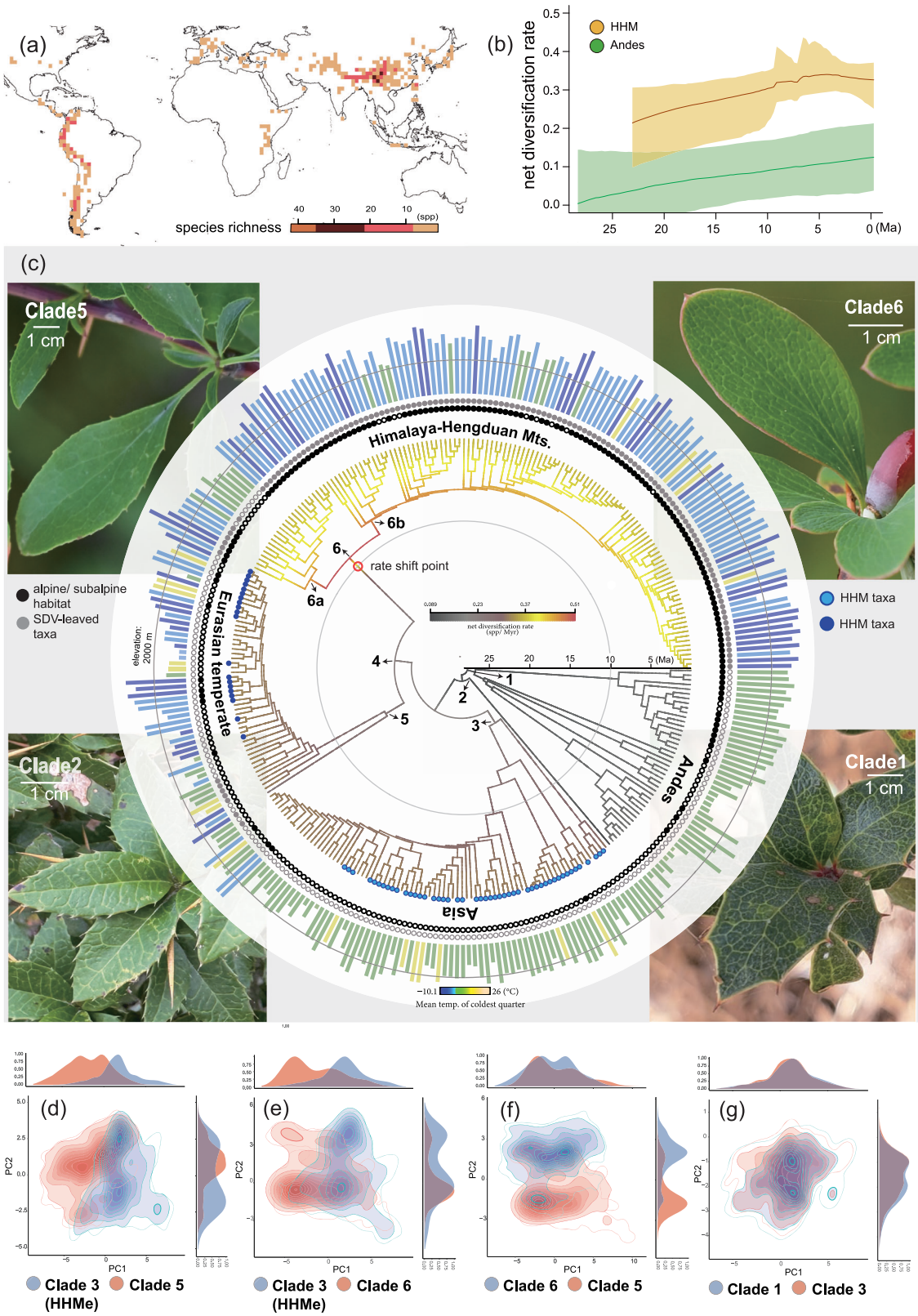

for in situ speciation and/or lineage immigration. Alternatively, diversification in both regions may have been similarly influenced by Neogene orogeny, which expanded montane biomes in the Andes and the HHM[5,16,17]. Higher richness in the HHM could instead reflect faster net diversification, perhaps enhanced by greater ecological opportunities[18,19]. For example, the HHM might offer greater habitat diversity or climatic niche space than the Andes. Ecological opportunity in this sense could have been influenced by the evolution of functional traits that expanded the fundamental niche, and/or by environmental change that reconfigured habitat availability and thereby expanded the realized niche[20,21].

The functional traits in *Berberis* that bear most directly in this context are those of leaves, which vary widely in size, shape, and vein density across species [22–24]; Supplementary Fig. 1). A conspicuous

Fig. 1 | Global diversification and geographic–ecological patterns of *Berberis*. **a** Species richness map of *Berberis*. **b** Diversification dynamics of *Berberis*, with the rate-through-time plot of net diversification rate across Andes and Hengduan-Himalaya Mts. (HHM) region. **c** A time-scaled phylogeny of *Berberis*. Clade 1: the Andean clade, Clade 2: the African clade, Clade 3: the Asian clade (species inhabiting the HHM regions are indicated by blue dots), Clade 4: the deciduous clade; Clade 5: the Eurasian temperate clade (species inhabiting the HHM regions are indicated by navy blue dots), Clade 6: deciduous clade mostly endemic to the HHM (6a: a Himalayan subclade, 6b: the Hengduan Mt. high-elevation subclade). The bar color shows the value of Bio 11 (mean temperature of coldest quarter), an indicator for cold hardiness. The bar length shows the median elevation of the species. At the genus level, the diversification rate shift point is indicated by the red hollow point in the Clade 6. The gray/ white dots beneath the elevation bar show species featuring small, densely veined (SDV) leaf (white: non-SDV leaved vs gray: SDV leaved), while the habitat type of species is indicated by black/ white boxes (black: alpine/ subalpine vs white: non-alpine/ non-subalpine). **d** Climatic niche comparison between the HHM-endemic evergreen species of Asian Clade 3 (HHMe) and the deciduous non-SDV Clade 5. **e** Comparison between the HHM-endemic evergreen species of Asian Clade 3 (HHMe) and the deciduous SDV Clade 6. **f** Comparison between the deciduous non-SDV Clade 5 and SDV Clade 6. **g** Comparison between the evergreen Andean Clade 1 and the evergreen Asian Clade 3. Density plots in PCA space illustrate patterns of climatic niche overlap and divergence among evergreen and deciduous clades. In each panel, contours represent kernel density estimates of species occurrences projected onto the first two principal components (PC1 and PC2), with marginal density plots showing univariate distributions along each axis. Source data are provided as a Source Data file. Photo credit: The photograph of *B. chilensis* in panel c is reproduced from an iNaturalist observation by Victor Pino Jofré (CC0 license). All other photographs in panel c were taken by the author.

contrast is that all species in the Andes are evergreen, whereas in the HHM, about 70% of the species are deciduous. The deciduous species are especially prevalent in the alpine and subalpine biomes (Supplementary Note 1), where about 85% of them are characterized by small, densely-veined (SDV) leaves (Supplementary Fig. 2). Outside the HHM, the deciduous-SDV condition is rare, leading us to hypothesize that it may represent a "key synnovation": a combination of traits whose joint effects, rather than any single trait alone, synergistically promote diversification[25]. Specifically, deciduousness can enhance nutrient resorption and facilitate rapid early-season carbon gain[26], small leaves can improve thermal balance and hydraulic stability[27,28], and high vein density can increase hydraulic safety and photosynthetic capacity ([29]; Supplementary Table 1). The evolution of deciduous–SDV leaves may thus have expanded the fundamental niche of *Berberis* to include colder and drier conditions, and enabled its radiation in alpine and subalpine habitats of the HHM.

To investigate this idea, a phylogeny of *Berberis* is necessary to establish when, where, and how fast diversification occurred, and to estimate the ancestral evolutionary sequences of key traits. Unfortunately, the fragmentary nature of the *Berberis* fossil records precludes the direct measurement of ancestral leaf functional traits, requiring statistical inference from extant species. Prior to this study, molecular phylogenies based on limited Sanger sequence data had determined the Andean species to be a monophyletic group, but did not resolve relationships of species in the HHM, the rest of Asia, North America, Europe, and Africa[30,31]. Here, our objectives are to resolve these relationships and relate the evolution of functional traits (deciduousness and SDV leaves) to rates of diversification and environmental change. Our study system allows phylogenetically controlled comparisons of diversification rate across regions (Andes vs HHM) and phenotypes. We are particularly interested in whether the deciduous-SDV condition evolved once or multiple times convergently, if deciduousness or SDV leaves evolved first, and what effect this combination of traits had on rates of diversification during time periods consistent with the expansion of high-elevation habitats in the HHM.

Results and discussion

We inferred the species-tree topology of *Berberis* from SNP variation across 3,175 orthologous genes using a coalescent-based approach in ASTRAL-IV (307 *Berberis* taxa and two outgroup taxa; Supplementary Note 2). This topology was then used as a constraint for divergence-time estimation, yielding a time-scaled phylogeny (Supplementary Fig. 3). It shows that *Berberis* diverged from its subtropical lowland sister lineage *Moranothamnus* about 29.9 Ma (early Oligocene). The topology contains a basal paraphyletic grade of evergreen lineages consisting of an Andean clade (Clade 1; crown age ~28 Ma), an African clade (Clade 2; stem age ~27.2 Ma), and an Asian clade (Clade 3; crown age ~22.7 Ma). The latter is sister to a large deciduous clade (Clade 4; crown age ~22.6 Ma). Ancestral state reconstruction shows that the genus was likely ancestrally evergreen (Fig. 2), with deciduousness a derived condition that evolved once along the stem of Clade 4 during the early Miocene (~22.6–20.4 Ma; Supplementary Fig. 4), likely within the HHM (Fig. 2; and Supplementary Fig. 5). Notably, this timing postdates the Oligocene–Miocene Transition and coincides with a period of oscillatory warming, rather than with major episodes of global Cenozoic cooling[32]. It is also considerably younger than the Late Cretaceous to Paleogene origins often inferred for deciduousness in other plant lineages, where the trait has been linked to adaptation to high-latitude darkness or strongly seasonal aridity[33,34]. Deciduousness in *Berberis* may therefore have evolved in response to regional rather than global climatic conditions[35], reflecting a lineage-specific adaptive trajectory potentially facilitated by local recruitment from lower-elevation environments into temperate and high-elevation habitats within the HHM. This scenario is consistent with fossil and tectonic evidence indicating that parts of the Hengduan Mountains (HDM) had reached near-modern elevations by the late Eocene, thereby providing early opportunities for adaptation to cold, high-elevation environments[36–38].

Within the deciduous Clade 4, SDV leaves evolved at least twice (Supplementary Fig. 6). They likely evolved once along the stem of the HHM-endemic Clade 6 (~ 20.4–9 Ma), in which 131 out of 138 have SDV leaves, and at least once in the Eurasian Clade 5, in which five out of the 50 species sampled have SDV leaves, all from the Mediterranean region (Fig. 1). The diversity of SDV-leaved species at high elevations in the HHM suggests that the combination of deciduousness and SDV leaves confers an adaptive advantage in alpine and subalpine environments. Niche analyses support this interpretation: deciduous species exhibit significantly greater cold hardiness than evergreens (Fig. 1; and Supplementary Figs. 7, 8), and within deciduous clades, SDV taxa occur at higher elevations (Fig. 1; and Supplementary Fig. 9) and in colder, less seasonal habitats of the HHM (Fig. 1; and Supplementary Figs. 7, 8). In contrast, the Andean and HHM evergreen lineages occupy largely similar climatic niches (Fig. 1), and within the HHM, non-SDV deciduous species track the elevational ranges of evergreens, shifting toward higher latitudes rather than into colder, higher-elevation habitats (Supplementary Fig. 10).

Estimates of speciation and extinction rates revealed higher net diversification in the HHM compared to the Andes (Fig. 1), with a significant shift toward faster diversification in Clade 6 around 10 Ma (late Miocene; Fig. 1). With the crown age of the Andean clade being older than that of the Asian clades (Clades 3 + 4), we can reject the null hypothesis that the richness of *Berberis* in the HHM simply reflects a longer time for speciation at constant rates. To test whether higher rates of diversification in the HHM are driven by trait-environment interactions, we fit two models of state-dependent diversification. The first showed that, across the phylogeny of *Berberis*, occurrence in montane habitats (versus non-montane; Supplementary Note 1) and being deciduous (versus evergreen) are each associated with higher

https://doi.org/10.1038/s41467-026-75790-3

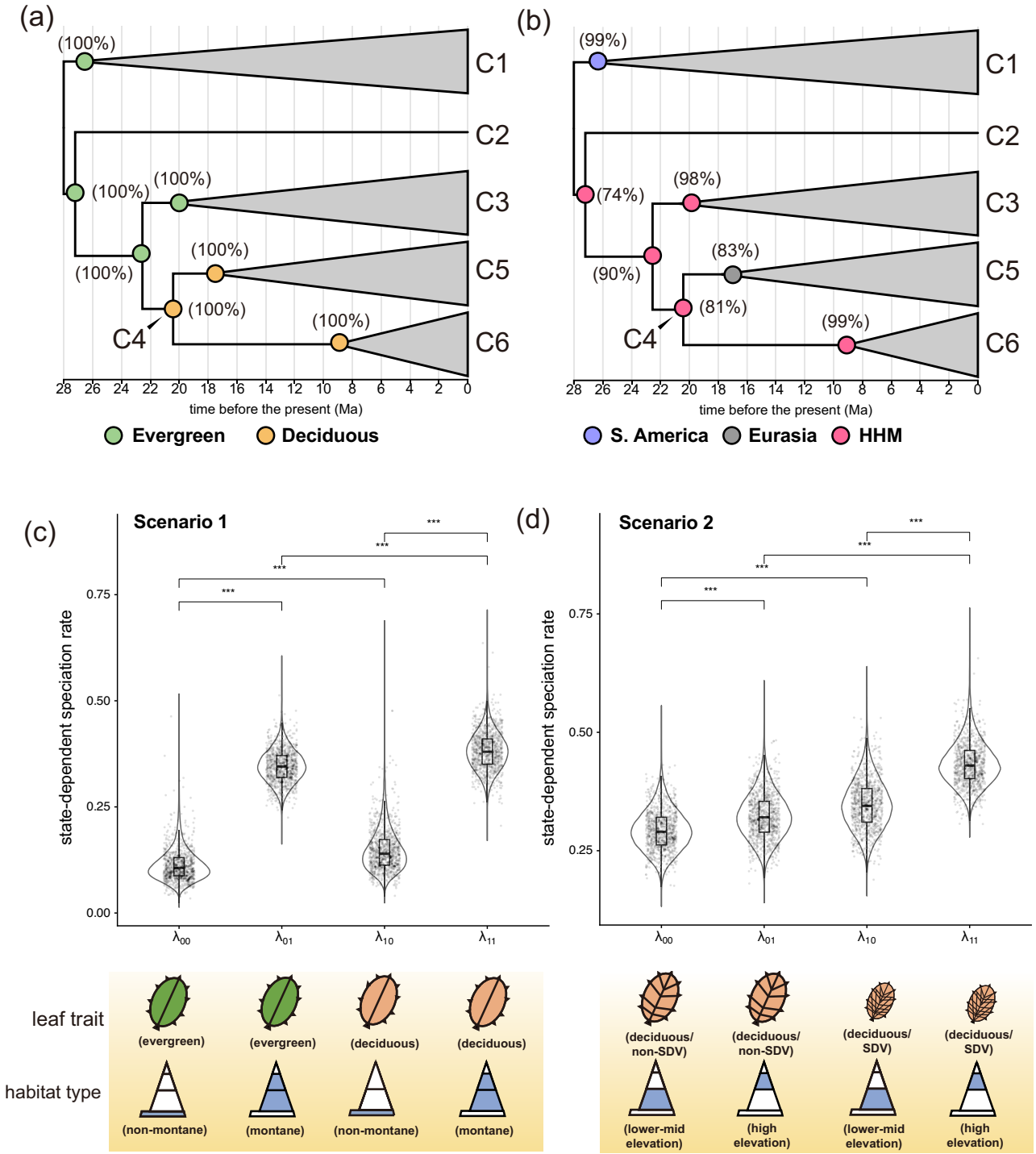

Fig. 2 | Evolutionary trajectory of leaf traits, geography, habitat type and their effects on speciation rates in *Berberis*. **a** Ancestral state reconstruction of deciduous and evergreen leaf habits. **b** Ancestral state reconstruction of geographic distributions. Colored circles represent the most probable ancestral state at each node, with values in parentheses indicating the corresponding probabilities. In **a**, orange denotes deciduousness and green denotes evergreen. In **b**, purple represents South America, pink denotes the HHM, and gray denotes Eurasia (excluding the HHM). "C" denotes clade. **c** Effects of montane habitat and deciduousness on speciation rates in *Berberis* (Scenario 1). **d** Effects of high-elevation habitat and SDV leaves on speciation rates within deciduous *Berberis* (Scenario 2; see "Methods"). Speciation rates for each trait–habitat combination were estimated using multi-character state-dependent speciation and extinction (MuSSE) models applied to 100 randomly sampled *Berberis* phylogenies. Box-and-whisker plots show the median, first and third quartiles, and 95% Bayesian credible intervals. Violin plots summarize posterior distributions of state-specific speciation rates. Each point represents one post-burn-in MCMC sample, and 37,500 posterior samples were retained for each state-specific speciation-rate estimate. Asterisks indicate significance levels from two-sided pairwise Welch t-tests among state-specific speciation-rate estimates without adjustment for multiple comparisons (***, $p < 0.001$). Full statistical results are provided in Supplementary Table 12, 13. Source data are provided as a Source Data file.

speciation rates, with the highest rate inferred for species that are both montane and deciduous (Fig. 2). Similarly, the second model showed that, within the deciduous Clade 4, occurring at high elevation and having SDV leaves are individually associated with higher speciation rates, with the highest rate associated with the combination of high-elevation and SDV leaves (Fig. 2). These results demonstrate a hierarchically nested, environment-dependent pattern in which the diversification effects of SDV leaves arise only within lineages that have previously evolved deciduousness, and that their sequential evolution represents a key synnovation, enabling the proliferation of *Berberis* species in successively higher-elevation habitats in the HHM.

The significantly elevated speciation rate associated with deciduous-SDV leaves in high-elevation habitats provides the first line of evidence that the synnovation of leaf traits enabled the expansion of the fundamental niche of *Berberis* and generated novel ecological opportunities in the HHM. A second line of evidence lies in the spatial and temporal confluence of trait evolution with environmental change. In the Himalayas, Neogene orogeny has been inferred to include uplift phases around 13 Ma and again between 10 and 5 Ma[39,40]. Likewise, recent tectonic reconstructions indicate that the HDM experienced continuous but heterogeneous deformation since the Eocene[41–43], including a period of rapid uplift in the middle Miocene (~10 Ma[37,44]), driven by orogenic activity along both the western and eastern margins of the range[45,46]. The timing of these geomorphological reorganizations closely aligns with the crown age of Clade 6 (~ 9 Ma) and an increase in diversification rates (Fig. 1). We therefore infer that, along the stem lineage leading to Clade 6, the evolution of SDV leaves coincided with increasing availability of alpine and subalpine environments, supporting the hypothesis that the confluence of functional innovation and ecological opportunity facilitated accelerated diversification[25].

The key synnovation of deciduous-SDV leaves in *Berberis* further illustrates how tectonically mediated restructuring of high-elevation habitats can act as an important extrinsic driver of diversification. Speciation in Clade 6 was likely promoted by the sky-island effect of allopatric isolation across valleys and high peaks[47,48], with intermittent reconnections during colder periods possibly facilitating the spread of adaptive alleles[49–51]. Such cycles of fragmentation and reconnection can promote ecological divergence among co-occurring lineages by reducing climatic niche overlap[52]. In particular, “flickering connectivity” in large mountain systems may generate repeated secondary contact[49,50], facilitating niche separation and lowering the likelihood of competitive exclusion, thereby contributing to the accumulation of species richness. In Clade 6, higher specie richness in the HDM than in the Himalayas suggests that differences in mountain hypsography may have influenced the capacity of these regions to generate and maintain species diversity[53]. The extensive area and north–south orientation of the HDM, in concert with intensified monsoon-driven river incision and relief development[54], likely generated steep environmental gradients and its characteristic mosaic of fragmented high-elevation landscapes characteristic of the modern HHM[55]. Moreover, during Pleistocene climatic oscillations, the complex topography of the HDM may have provided more extensive refugial habitats, facilitating lineage persistence relative to the Himalayas[9]. Whether SDV leaves represent an adaptation to high-elevation habitats in the HDM (i.e., they evolved by natural selection in response to such environments) is difficult to ascertain, since it is possible that SDV leaves originated as early as the stem age of Clade 6, ~20.4 Ma (Fig. 2), when alpine habitats were relatively restricted. In either case, the confluence of functional innovations and abiotic environmental change illustrates the context-dependent nature of macroevolutionary shifts in lineage diversification. A limitation of the present study is that the genetic basis of the deciduous–SDV syndrome remains unresolved; future transcriptomic and comparative genomic analyses will be necessary to link these traits to their underlying regulatory and developmental mechanisms[56].

In light of patterns in the HDM, the slower diversification inferred in the Andean clade may reflect macroevolutionary dynamics shaped by different topographic and climatic histories, potentially interacting with the absence of the deciduous-SDV synnovation (Fig. 1). Compared to deciduous lineages, the environmental niche of the evergreen Andean clade is restricted to warmer conditions, which likely limited its capacity to colonize alpine zones formed during Late Neogene uplift in the northern and central Andes[6,17]. Global Neogene cooling appears to have similarly constrained diversification in evergreen lineages such as *Caragana* and *Ilex*[57,58]. Consistent with this interpretation, environment-dependent diversification analyses revealed a significant association between speciation rates (Supplementary Fig. 11) and declining paleotemperatures since the Oligocene for evergreen lineages in both the South American Andes and the HHM.

If deciduousness and SDV leaves had evolved in the Andes, would diversification rates have responded similarly as in the HHM? To investigate this, we projected the climatic niches of the evergreen Andean Clade 1 and deciduous Clade 4 onto a paleoclimate model spanning the Neogene of South America (Fig. 3). The niche modeling indicated extensive potential habitat for Clade 4 in the Oligocene and Miocene with significant contraction toward the present covering regions that today harbor few, if any, species of *Berberis* (~30°S–40°S). By contrast, niche models of the Andean Clade 1 showed a long-term restricted distribution in S. America (Fig. 3), disconnected from the potential distribution of deciduous *Berberis*. Moreover, the projected niche model of the deciduous-SDV leaved Clade 6 covers an area of S. America significantly smaller than its natural range in the HHM (Supplementary Fig. 12). Here, projections of HHM deciduous lineages are used to approximate environmental conditions favorable to this trait combination, rather than to infer their historical presence in South America. These results suggest that deciduousness could indeed have facilitated a fundamental niche shift in Andean *Berberis*, providing the evolutionary potential for diversification into newly formed montane habitats created by Andean uplift. However, the subsequent evolution of SDV leaves—while paralleling the trajectory observed in the HHM—would likely not have triggered a radiation of comparable scale, because potential habitats for deciduous lineages in the Andes contracted substantially through time and are now highly restricted. In contrast, comparable contractions were not inferred for the HHM, where the potential habitat of deciduous Clade 4 persisted or expanded during the Neogene (Fig. 3; and Supplementary Fig. 12). These contrasts also suggest that the Andes and the HHM differ not only in the temporal dynamics of habitat availability, but also in the environmental context shaping trait evolution and lineage diversification.

Methods

Ethics statement

Wild collections conducted for this study did not involve protected species, nationally protected plants, or plant species with extremely small populations, nor were they conducted within national parks or the core zones of protected areas. Under these circumstances, specific collection permits were not required. Prior to each field survey, the relevant local authorities were notified through formal letters of introduction issued by the Xishuangbanna Tropical Botanical Garden (XTBG), Chinese Academy of Sciences. A complete list of sampling metadata is provided in the Sampling Metadata file available in the folder “0. Species distribution, habitat and sampling” at (https://doi.org/10.6084/m9.figshare.28288313).

Genomic data processing and phylogenomic inference

We sampled 307 *Berberis* taxa, representing ~65% of the described species diversity within the genus sensu stricto[31]. Across the Andes and the HHM, our sampling encompassed ~62% of the species known from these regions (Supplementary Table 2). Distributional records were validated to exclude cultivated or misidentified accessions. Putative

https://doi.org/10.1038/s41467-026-75790-3

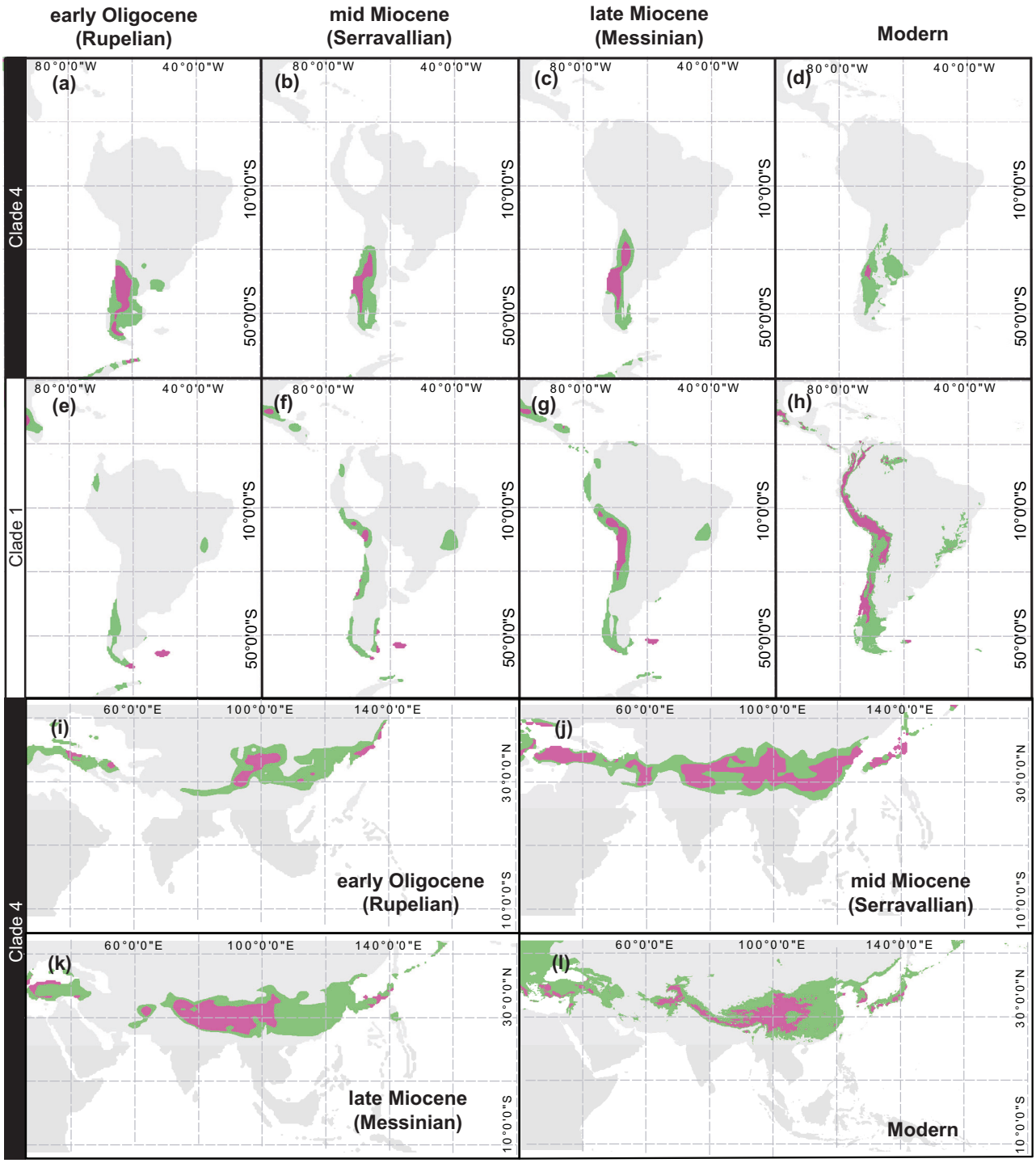

Fig. 3 | The estimated present and past ranges of deciduous and evergreen *Berberis* in South America and Asia. a–c show the predicted climatic niche distributions of deciduous Clade 4 in South America across three geological periods, and panel (**d**) shows the corresponding present-day distribution. **e–g** show the predicted climatic niche distributions of Andean Clade 1 across three geological periods, with **h** showing the corresponding present-day distribution. **i–k** show the predicted climatic niche distributions of deciduous Clade 4 in Asia across three geological periods, and **l** shows the corresponding present-day distribution. Relative habitat suitability is classified as moderate (0.4–0.7; green) and high (0.7–0.9; pink-red). Source data are provided as a Source Data file.

single-copy orthologs were identified using OrthoFinder v2.5.5[59] based on protein-coding sequences from four reference genomes, retaining orthogroups that contained simply one gene per genome for downstream phylogenomic analyses. Total genomic DNA was extracted from leaves dried with silica gel, using a modified CTAB procedure. About 6–15 Gb of genomic data were generated by an Illumina NovaSeq 6000 platform with a reading length of 150 bp. For variant calling, whole-genome resequencing data from 307 *Berberis* accessions were quality-filtered using fastp v0.23.2 with default parameters[60]. High-quality reads were aligned to the reference genome using BWA-MEM v0.7.17[61], and the resulting BAM files were sorted with SAMtools v1.15.1[62]. SNPs were called with bcftools (v1.17) mpileup and call modules, merged, and filtered with a minor allele frequency (MAF) threshold of 0.05 to produce the initial genome-wide SNP dataset

(Dataset 1). Dataset 1 is not distributed directly but can be regenerated from the deposited resequencing data by following the README provided in the folder "1. Phylogenomic inference" at (https://doi.org/10.6084/m9.figshare.28288313). Based on the annotation of the reference genome, we retrieved the coordinates of 3,175 predicted single-copy genes and used bcftools to extract SNPs within these regions, generating the orthologous-gene SNP dataset (Dataset 2), which is available in the folder "1. Phylogenomic inference" at (https://doi.org/10.6084/m9.figshare.28288313). Species with >50% missing SNPs were excluded, resulting in alignments for 1,740 genes, each containing 10–30 SNPs. Gene trees for each locus were reconstructed using IQ-TREE3[63] under the maximum likelihood framework, with model selection performed using the MFP + ASC option and branch support assessed via 1000 ultrafast bootstrap replicates. Consensus trees were processed with Newick Utilities to collapse nodes with bootstrap support <10%, following the recommendations of the ASTRAL manual[64]. These gene trees were then used as input for ASTRAL-IV[65,66] to estimate a species tree with branch lengths, which was subsequently rooted using *Mahonia*. Local posterior probabilities (LPP) were calculated to assess node support.

Divergence time estimation

Divergence times were estimated using the IQ2MC pipeline[67], which integrates gene tree inference in IQ-TREE3 and species tree dating in MCMCTree[68]. The ASTRAL species tree was used as a fixed constraint topology in MCMCTree. Analyses were performed in PAML 4.10.8.iq2mc under an independent-rates relaxed clock model (clock = 2). Site-wise log-likelihoods and Hessian matrices for each gene alignment were precomputed in IQ-TREE3 (usedata = 2) to enable approximate likelihood computation in MCMCTree. A birth–death process was specified as the tree prior (BDparas = 1 1 0). The mean substitution rate across loci followed a gamma prior (rgene_gamma = 2 400), and rate variance among lineages followed a gamma prior (sigma2_gamma = 1 10). Two independent MCMC chains of 500,000 generations each were run, discarding the first 200,000 as burn-in and sampling every 700 generations. Convergence was assessed by examining trace plots and effective sample sizes (ESS > 200) in TRACER v1.7.2[69]. Posterior samples of divergence times were used to generate a set of 100 time-calibrated trees for downstream analyses. Three fossil calibrations were applied to constrain node ages: (i) the stem age of *Mahonia* was set to 47.8 Ma based on the middle Eocene fossil *M. marginata*[70]; (ii) the crown age of *Berberis* Clade 5 was set to 28.4 Ma from the early Miocene leaf fossil *B. berberidifolia*[71]; and (iii) the crown age of Chilean taxa of the Clade 1 was constrained to 23 Ma using the Oligocene fossil *B. lozanofolia*[72].

Trait measurement and ancestral state reconstruction

Leaf area (LA) and major vein length—defined as the density of primary and secondary veins[29]—were measured from scanned images using ImageJ2[73]. Major vein length density (MVD, i.e., total vein length per unit area) was calculated by dividing major vein length (cm) by leaf area (cm^2). For each species, three herbarium specimens were measured whenever available. Within each specimen, 1–3 fully expanded and undamaged leaves were selected for analysis to minimize sampling bias. In cases where only a type specimen or limited material was available, measurements were based on the maximum number of intact leaves suitable for analysis, which in rare cases was a single leaf. A pretest comparing herbarium and fresh material from eight species across four major clades (Clades 1, 3, 5, and 6) showed no significant differences in LA or MVD, validating the use of herbarium material. A Welch two-sample t-test was used to assess whether leaf traits (LA, MVD) and the mean temperature of the coldest quarter differed among the major clades shown in Fig. 1 and Supplementary Fig. 1. Ancestral states of leaf habit and habitat of *Berberis* were reconstructed using stochastic character mapping implemented in the R package 'phytools'[74]. We performed 1000 simulations under the equal-rates (ER) model using the function make.simmap, generating posterior probabilities of character states for each node based on the time-scaled phylogeny. For state-dependent speciation and extinction (SSE) analyses, continuous data for LA and MVD were discretized into binary states using the R package 'discretization', which applies chi-square and decision-tree criteria. The cutoff for LA was set at 4.48 cm^2, classifying values below this threshold as "small" leaves (Supplementary Fig. 10), consistent with[27]. The cutoff for MVD was set at 5.48 cm, with values below this threshold classified as "low" MVD. In this study, SDV leaves were defined as those combining small LA and high MVD.

Macroevolutionary rates and biogeographic analysis

To investigate speciation rate variation over time across *Berberis* lineages, we used a time-dependent Bayesian model in Bayesian Analysis of Macroevolutionary Mixtures (BAMM 2.5.0[75,76]). Prior values for rate parameters were set using the setBAMMpriors function. We tested priors for the expected number of diversification rate shifts (0.1, 0.5, 1, 5, and 10) and ran two Markov Chain Monte Carlo (MCMC) chains of 50 million steps each to ensure reciprocal convergence. Single-chain convergence was assessed using the ESS with a minimum threshold of 200. We incorporated a non-random incomplete taxon sampling approach to account for the varying number of included taxa in different clades of *Berberis*, with an overall sampling fraction of 0.65. The statistical support for the number of diversification rate shifts was evaluated based on the Posterior Probability (PP) after discarding 25% of the posterior samples as burn-in. Ancestral range estimation was performed in BioGeoBEARS[77] under the Dispersal–Extinction–Cladogenesis (DEC) model of geographic range evolution[78]. We optimized dispersal (d) and extinction (e) parameters on the time-calibrated species tree. Biogeographic areas were defined as South America, Africa, North America, Eurasia (excluding the HHM region), and the HHM. To account for temporal changes in continental connectivity, and the climatic niche of *Berberis*, we implemented a dispersal-constrained DEC model with three time-stratified intervals (T1: before 30 Ma; T2: 30–5 Ma; T3: 5–0 Ma; Table S8). Before the Oligocene (T1), Earth was in a greenhouse climatic phase[32] and the Tethys Ocean remained a barrier between Europe and Asia. Accordingly, dispersal between these regions was set to a relatively low value. Between the Oligocene and late Miocene (T2), the climate was comparatively stable[32], but the Central American Seaway still limited exchange between North and South America and the North Atlantic land bridge had weakened. Thus, dispersal among these regions was reduced relative to adjacent areas. After the late Miocene (T3), the global climate became cooler and more seasonal[32], likely further restricting exchange among northern temperate regions. Therefore, dispersal probabilities between North America, Europe, and Asia were further reduced. Dispersal between nonadjacent regions was set to low baseline values across all time slices.

Trait dependent diversification

To evaluate how biotic traits (deciduousness and SDV leaves) and abiotic factors (montane and high-elevation habitats; Supplementary Note 2) influence speciation in *Berberis*, we used state-dependent speciation and extinction (SSE) models to test trait- and environment-dependent diversification (Supplementary Table 3). Because the effect of any given trait may depend on its interaction with other traits or environmental contexts, we examined two complementary diversification scenarios. Scenario 1 evaluated the joint effects of deciduousness and montane habitat on speciation across the genus, whereas Scenario 2 focused on the effects of high-elevation habitat and SDV leaves within the deciduous Clade 4. To determine whether speciation rates vary with unmeasured traits rather than selected traits and

habitats, we first fitted our trait and habitat datasets to multistate SSE models with hidden states using the R package 'MuHiSSE'[79]. In this approach, hidden characters represent unmeasured factors potentially influencing speciation rates. Specifically, we tested eight models (Supplementary Table 4, 5): (i) three MuSSE-like models without hidden states; (ii) two trait-dependent MuHiSSE models with two and three hidden states; and (iii) three character-independent diversification (CID) models with increasing numbers of hidden states. We compared the likelihood of eight candidate models with increasing complexity. Model support was primarily evaluated using an information-theoretic framework based on AICc values, ΔAICc, and Akaike weights. Since the MuHiSSE results rejected the hidden-state models in both Scenario 1 & 2 (Supplementary Table 6, 7), we proceeded to fit our data to a multi-character SSE model without hidden states using the R package 'MuSSE'[80]. This approach allowed us to quantify the 'additive' and 'interactive' effects of any two binary traits on diversification, following ([81]; Supplementary Table 8). To focus on the evolution of deciduousness and montane habitat, we defined *Berberis* species that are neither deciduous nor montane as the 'base' trait-habitat state in this case, according to the MuSSE user manual[80]. Accordingly, additive effects of deciduousness or montane habitat on speciation rates were calculated as differences in estimated rates between *Berberis* taxa in the base state and those with the deciduousness or montane habitat. Interactive effects on speciation were similarly calculated by comparing taxa with both traits to those without them. By doing this, we aim to disentangle how a single or a particular trait/ habitat combination affects the speciation rate of *Berberis* in both Scenarios 1 & 2. Specifically, we applied this model to calculate the speciation rates of four trait-habitat combinations in Scenario 1 (evergreen/ non-montane, evergreen/ montane, deciduous/ non-montane, deciduous/ montane), and another four in Scenario 2 (deciduous non-SDV/ lower-mid elevation, deciduous non-SDV/ high-elevation, deciduous SDV/ lower-mid elevation, deciduous SDV/ high-elevation). In Scenario 1, the base state in *Berberis* is defined by species that are evergreen and do not occur in montane region, while in scenario 2 the base state of deciduous *Berberis* indicates species without SDV leaf and occur in the lower-mid elevation. We implemented MuSSE to quantify trait-dependent diversification for the above eight trait/ habitat combinations (Supplementary Table 9). Model support was primarily evaluated using an information-theoretic framework based on AICc values, ΔAICc, and Akaike weights. For nested model comparisons, likelihood ratio tests were additionally conducted using the *anova* function in the R package 'diversitree' to assess whether models with additional parameters provided a significantly better fit than simpler alternatives ($p < 0.05$). For the best-supported MuSSE model, Bayesian parameter estimation was performed using MCMC in the *diversitree* framework across 100 randomly sampled phylogenetic trees to incorporate topological and branch-length uncertainty. For each tree, short pilot chains were first used to optimize proposal widths, followed by the main posterior sampling run. Posterior samples from each tree were first summarized by their mean state-specific diversification rates. The resulting tree-level estimates were then used to characterize the distributions of diversification rates across the 100 sampled trees. Differences among states were evaluated using two-sided pairwise Welch t-tests comparing tree-level state-specific speciation-rate estimates. Model comparison results for Scenario 1 and Scenario 2 are summarized in Supplementary Tables 10 and 11.

Paleoenvironment dependent diversification

We estimated temporal variation in diversification rates under a Bayesian environment-dependent model implemented in RevBayes v1.3.1[82]. The time-calibrated phylogeny was analyzed using an episodic birth–death framework, in which speciation and extinction rates were allowed to vary among time intervals in response to changes in paleotemperature. Ancient temperature data were compiled from[83] and aligned with the temporal bins of the phylogeny. Changes in temperature between consecutive intervals were used as the environmental predictor influencing diversification rates. We specified weakly informative priors on all rate parameters and included the empirical taxon-sampling fraction to correct for incomplete sampling. The model was run in two independent Markov chain Monte Carlo (MCMC) analyses, each for 2 million generations, sampling every 500 steps and discarding the first 25 % as burn-in. Posterior estimates of the correlation coefficients between diversification rates and paleo temperature were summarized to evaluate the direction and strength of environmental dependence (Supplementary Fig. 11). All analyses were performed in RevBayes, and posterior summaries plots were generated using the RevGadgets R package[84].

Ecological niche divergence analysis

We used the environmental (E)-space–based framework implemented in the R package HUMBOLDT[85] to quantify climatic niche overlap and divergence among major *Berberis* clades based on the present phylogeny. Specifically, we conducted a series of niche comparisons between HHM-endemic evergreen (HHMe) species of the Clade 3 and the Clade 5; between the HHMe of the Clade 3 and the Clade 6; between the Clade 5 and Clade 6, and between the Clade 1 and Clade 3 (Fig. 1). Nineteen bioclimatic variables (Bio1–Bio19) at 30 arc-second resolutions were obtained from CHELSA-W5E5 for current climatic conditions[86], with potential evapotranspiration (PET) included to capture variation in atmospheric evaporative demand relevant to plant water balance. Highly correlated variables (Pearson's $r > |0.75|$) were removed using ENMTOOLS v1.4.4 in R to minimize multicollinearity and model overfitting[87]. A principal component analysis (PCA) in E-space was performed using eight retained environmental variables: Bio1 (annual mean temperature), Bio2 (mean diurnal temperature range), Bio3 (isothermality), Bio4 (temperature seasonality), Bio12 (annual precipitation), Bio14 (precipitation of the driest month), Bio15 (precipitation seasonality), and PET. Environmental niche occupancy for each clade (i.e., Clade 1, 3, 4, 5, 6 and HHMe of the Clade 3) was quantified directly in environmental-space (i.e., E-space). Kernel density estimates in E-space were used to visualize the two-dimensional distribution of climatic conditions. Niche similarity between clades was then evaluated using the niche overlap test (NOT) and niche differentiation test (NDT) implemented in HUMBOLDT[85], with equivalency (E) and background (B) statistics calculated from 500 replicates. NOT assesses whether two clades occupy statistically equivalent environmental distributions across the full E-space, whereas NDT tests for significant differentiation within the portion of E-space shared by both clades. In both tests, the E statistic compares the observed Schoener's D value[88] with a null distribution generated by resampling and spatially shifting occurrences, while the B statistic evaluates whether the observed D differs from expectations given environmental differences between regions. Because these analyses operate directly on realized climatic distributions rather than on inferred ancestral niches, we use the term 'niche differentiation' to describe significant differences in climatic occupancy between clades.

Present and past distribution modeling of deciduous and evergreen *Berberis* in S. America

We used Maximum Entropy modeling (MaxEnt, v3.4.4[89];) to simulate the potential distributions of deciduous and evergreen *Berberis* in South America across present and past periods, based on 1,352 distribution records. Nineteen bioclimatic variables (Bio1–Bio19) at 30 arc-second resolution were obtained from CHELSA-W5E5 for current climatic conditions, with potential evapotranspiration (PET) included to capture variation in atmospheric evaporative demand relevant to plant water balance. To reconstruct the climatic niche envelopes of Andean Clade 1, deciduous Clade 4, and the HHM deciduous Clade 6, we used the same eight climatic variables and data pipeline as in the

niche overlap analysis. We then projected each clade's reconstructed niche envelope onto present day South America and Asia, and across three geological periods: early Oligocene (Rupelian), mid Miocene (Serravallian), and late Miocene (Messinian), using paleoclimate data simulated with HadCM3LB-M2.1D[90]. The model simulates climate across geological time by incorporating boundary conditions and physical processes, in which the land-sea boundaries, elevations, and ice sheets are based on paleogeographic data[91]. Atmospheric CO_2 concentrations were revised and set following data[92]. For both past and present modeling, we randomly selected 75% of distribution data as training data, with 25% for testing, and performed cross-validation with 10 replicates. Model performance was evaluated using the AUC metric, where AUC > 0.9 indicates high predictive performance. We also used a jackknife test to assess the relative importance of environmental variables. The MaxEnt output, converted to raster format, classified habitat suitability into moderate (0.4–0.7, greenish) and high (0.7–0.9, pinkish-red) levels.

Data availability

Raw sequencing reads and genome assemblies generated in this study have been deposited in the NCBI database under BioProject accession PRJNA1457873. The four genome assemblies are also available through DDBJ/ENA/GenBank under Whole Genome Shotgun accessions JBYVFI000000000, JBYVFJ000000000, JBYVFK000000000, and JBYVFL000000000; the versions described in this paper are JBYVFI010000000, JBYVFJ010000000, JBYVFK010000000, and JBYVFL010000000. Processed SNP datasets, gene alignments, phylogenetic trees, and additional analysis outputs supporting the findings of this study are available at Figshare (https://doi.org/10.6084/m9.figshare.28288313). Source data are provided with this paper.

Code availability

The scripts used for the analyses conducted in this study are available through GitHub and archived in *Zenodo* at (https://doi.org/10.5281/zenodo.20526753).

References

1. Perrigo, A., Hoorn, C. & Antonelli, A. Why mountains matter for biodiversity? *J. Biogeogr.* **47**, 315–325 (2020).
2. Rahbek, C. et al. Humboldt's enigma: what causes global patterns of mountain biodiversity? *Science* **365**, 1108–1113 (2019a).
3. Cao, G. L. et al. Cenozoic geoclimatic changes drove the evolutionary dynamics of floristic endemism on the Qinghai-Tibet Plateau. *Proc. Natl. Acad. Sci. USA* **122**, e2426017122 (2025).
4. Ding, W.-N., Ree, R. H., Spicer, R. A. & Xing, Y.-W. Ancient orogenic and monsoon-driven assembly of the world's richest temperate alpine flora. *Science* **369**, 578–581 (2020).
5. Xing, Y.-W. & Ree, R. H. Uplift-driven diversification in the Hengduan Mountains, a temperate biodiversity hotspot. *Proc. Natl. Acad. Sci. USA* **114**, e3444–e3451 (2017).
6. Testo, W. L., Sessa, E. & Barrington, D. S. The rise of Andes promoted rapid diversification in Neotropical *Phlegmariurus* (Lycopodiaceae). *N. Phytol.* **222**, 11–13 (2018).
7. Lagomarsino, L. P., Condamine, F. L., Antonelli, A., Mulch, A. & Davis, C. C. The abiotic and biotic drivers of rapid diversification in Andean bellflowers (Campanulaceae). *N. Phytol.* **210**, 1430–1442 (2016).
8. Zhang, X. et al. Macroevolutionary pattern of *Saussurea* (Asteraceae) provides insights into the drivers of radiating diversification. *Proc. Biol. Sci.* **288**, 20211575 (2021).
9. Muellner-Riehl, A. N. et al. Origins of global mountain plant biodiversity: testing the 'mountain-geobiodiversity hypothesis'. *J. Biogeogr.* **46**, 2826–2838 (2019).
10. Wootton, L. M. et al. The late rise of sky-island vegetation in the European Alps. *Nat. Plants*. **11**, 1142–1153 (2025).
11. Dellinger, A. S., Lagomarsino, L., Michelangeli, F., Dullinger, S. & Smith, S. D. The sequential direct and indirect effects of mountain uplift, climatic niche, and floral trait evolution on diversification dynamics in an Andean plant clade. *Syst. Biol.* **73**, 594–612 (2024).
12. Bastida, J. M., Alcántara, J. M., Rey, P. J., Vargas, P. & Herrera, C. M. Extended phylogeny of *Aquilegia*: the biogeographical and ecological patterns of two simultaneous but contrasting radiations. *Plant Syst. Evol.* **284**, 171–185 (2010).
13. Alencar, L. R. V. et al. Opportunity begets opportunity to drive macroevolutionary dynamics of a diverse lizard radiation. *Evol. Lett.* **8**, 623–637 (2024).
14. Henao-Diaz, L. F., Harmon, L. J. & Sugawara, M. T. C. Macroevolutionary diversification rates show time dependency. *Proc. Natl. Acad. Sci. USA* **116**, 7403–7408 (2019).
15. Vasconcelos, T. N. C. et al. Fast diversification through a mosaic of evolutionary histories characterized the endemic flora of ancient Neotropical mountains. *Proc. Biol. Sci.* **287**, 20192933 (2020).
16. Hughes, C. E. & Atchison, G. W. The ubiquity of alpine plant radiations: from the Andes to the Hengduan Mountains. *N. Phytol.* **207**, 275–282 (2015).
17. Pérez-Escobar, O. A. et al. The Andes through time: evolution and distribution of Andean floras. *Trends Plant Sci.* **27**, 364–378 (2022).
18. Simpson, G. G. et al. *The Major Features of Evolution*. (Columbia University Press, 1953).
19. Liu, J. Q., Wang, Y. J., Wang, A. L., Hideaki, O. & Abbott, R. J. Radiation and diversification within the *Ligularia–Cremanthodium–Parasenecio* complex (Asteraceae) triggered by uplift of the Qinghai-Tibetan Plateau. *Mol. Phylogenet. Evol.* **38**, 31–49 (2006).
20. Li, Y. et al. Accelerated speciation in temperate Cannabaceae: The role of pre-adaptation, ecological opportunities and niche divergence. *Glob. Ecol. Biogeogr.* **34**, e70183 (2025).
21. Chen, Y. P. et al. Rapid radiation of a plant lineage sheds light on the assembly of dry valley biomes. *Mol. Biol. Evol.* **42**, msaf011 (2025).
22. Ahrendt, L. W. A. *Berberis* and *Mahonia*: a taxonomic revision. *J. Linn. Soc. Bot.* **57**, 1–410 (1961).
23. Landrum, L. R. Revision of *Berberis* (Berberidaceae) in Chile and adjacent Southern Argentina. *Ann. Mo Bot. Gard.* **86**, 793–834 (1999).
24. Harber, J. *The Berberis of China and Vietnam: A Revision*. *Monogr. Syst. Bot. Mo. Bot. Gard.* **136**, 1–359 (2020).
25. Donoghue, M. J. & Sanderson, M. J. Confluence, synnovation, and depauperons in plant diversification. *N. Phytol.* **207**, 260–274 (2015).
26. Bai, K., He, C., Wan, X. & Jiang, D. Leaf economics of evergreen and deciduous tree species along an elevational gradient in a subtropical mountain. *AoB PLANTS* **7**, plv064 (2015).
27. Wright, I. J. et al. Global climatic drivers of leaf size. *Science* **357**, 917–921 (2017).
28. Lusk, C. H. et al. Frost and leaf-size gradients in forests: global patterns and experimental evidence. *N. Phytol.* **219**, 565–573 (2018).
29. Sack, L. & Scoffoni, C. Leaf venation: structure, function, development, evolution, ecology and applications in the past, present and future. *N. Phytol.* **198**, 983–1000 (2013).
30. Adhikari, B., Milne, I. R., Pennington, R. T., Särkinen, T. & Pendry, C. A. Systematics and biogeography of *Berberis* s.l. inferred from nuclear ITS and chloroplast ndhF gene sequences. *Taxon* **64**, 39–48 (2015).
31. Hsieh, C.-L., Yu, C.-C., Huang, Y.-L. & Chung, K.-F. *Mahonia* vs. *Berberis* unloaded: generic delimitation and infrafamilial classification of Berberidaceae based on plastid phylogenomics. *Front Plant Sci.* **12**, e720171 (2022).
32. sZachos, J., Pagani, M., Sloan, L., Thomas, E. & Billups, K. Trends, rhythms, and aberrations in global climate 65 Ma to present. *Science* **292**, 686–693 (2001).

33. Wolfe, J. A. & Upchurch, G. R. Vegetation, climatic and floral changes at the Cretaceous-Tertiary boundary. *Nature* **324**, 148152 (1986).
34. Röhrig, E. et al. *Floral composition and evolutionary development*. In *Temperate deciduous forests* (eds Röhrig, E. & Ulrich, B.) 17–23 (Elsevier, 1991).
35. Edwards, E. J. et al. Convergence, consilience, and the evolution of temperate deciduous forest. *Am. Nat.* **190**, S87–S104 (2017).
36. Su, T. et al. Uplift, climate and biotic changes at the Eocene-Oligocene transition in south-eastern Tibet. *Natl. Sci. Rev.* **6**, 495–504 (2019).
37. Li, S. et al. An updated chronostratigraphic framework for the Cenozoic sediments of the southeast margin of the Tibetan Plateau: Implications for regional tectonics. *Glob. Planet Change* **236**, 104436 (2024).
38. Spicer, R. A. et al. Why "the uplift of the Tibetan Plateau" is a myth. *Natl. Sci. Rev.* **8**, nwaa091 (2021).
39. Ding, L. et al. Quantifying the rise of the Himalaya orogen and implications for the South Asian monsoon. *Geology* **45**, 215–218 (2017).
40. Kapp, P. & DeCelles, P. G. Mesozoic–Cenozoic geological evolution of the Himalayan–Tibetan orogen and working tectonic hypotheses. *Am. J. Sci.* **319**, 159–254 (2019).
41. Ouimet, W. et al. Regional incision of the eastern margin of the Tibetan Plateau. *Lithosphere* **2**, 50–63 (2010).
42. DeCelles, P. G., Kapp, P., Gehrels, G. E. & Ding, L. Paleocene–Eocene foreland basin evolution in the Himalaya of southern Tibet and Nepal: Implications for the age of initial India–Asia collision. *Tectonics* **33**, 824–849 (2014).
43. Spicer, R. A. et al. The topographic evolution of the Tibetan Region as revealed by palaeontology. *Palaeobiodivers Palaeoenviron* **101**, 213–243 (2021).
44. Miao, Y. et al. A new biologic paleoaltimetry indicating late Miocene rapid uplift of the northern Tibetan Plateau. *Science* **378**, 1074–1079 (2022).
45. Chang, Y. et al. Tectonic and climatic controls on plant biodiversity in the Hengduan Mountains, China. *Geol. Soc. Lond. Spec. Publ.* **549**, 205–225 (2024).
46. He, J. et al. A comprehensive interpretation of thermochronological data in the Hengduan Mountains with tectonic implications. *Earth-Sci. Rev.* **271**, 105296 (2025).
47. Marx, H. E. et al. Riders in the sky (islands): using a mega-phylogenetic approach to understand plant species distribution and coexistence at the altitudinal limits of angiosperm plant life. *J. Biogeogr.* **44**, 2618–2630 (2017).
48. Steinbauer, M. J. et al. Topography-driven isolation, speciation and a global increase of endemism with elevation. *Glob. Ecol. Biogeogr.* **25**, 1097–1107 (2016).
49. Flantua, S. G. A. & Hooghiemstra, H. Historical connectivity and mountain biodiversity. In *Mountains, Climate and Biodiversity* (eds Hoorn, C., Perrigo, A. & Antonelli, A.) 171–185 (Wiley Blackwell, 2018).
50. Nevado, B., Contreras-Ortiz, N., Hughes, C. & Filatov, D. A. Pleistocene glacial cycles drive isolation, gene flow and speciation in the high-elevation Andes. *N. Phytol.* **219**, 779–793 (2018).
51. Flantua, S. G. A., O'Dea, A., Onstein, R. E., Giraldo, C. & Hooghiemstra, H. Snapshot isolation and isolation history challenge the analogy between sky islands and oceanic islands. *Glob. Ecol. Biogeogr.* **29**, 1523–1536 (2020).
52. Kandziora, M. et al. The overlooked link between different resource partitioning strategies and plant species richness in tropical alpine ecosystems. *Glob. Ecol. Biogeogr.* **34**, e70169 (2025).
53. Elsen, P. R. & Tingley, M. W. Global mountain topography and the fate of montane species under climate change. *Nat. Clim. Change* **5**, 772–776 (2015).
54. Wu, F. et al. Reorganization of Asian climate in relation to Tibetan Plateau uplift. *Nat. Rev. Earth Environ.* **3**, 684–700 (2022).
55. Nie, J. et al. Rapid incision of the Mekong River in the middle Miocene linked to monsoonal precipitation. *Nat. Geosci.* **11**, 944–948 (2018).
56. Zhang, Z. et al. Ancient hybridization underlies tuberization and radiation of the potato lineage. *Cell* **188**, 5249–5265.e15 (2025).
57. Zhang, M.-L., Xiang, X.-G., Xue, J.-J., Sanderson, S. C. & Fritsch, T. W. Himalayan uplift shaped biomes in Miocene temperate Asia: evidence from leguminous *Caragana*. *Sci. Rep.* **6**, 36528 (2016).
58. Yao, X., Song, Y., Yang, J.-B., Tan, Y.-H. & Corlett, R. T. Phylogeny and biogeography of the hollies (*Ilex* L., Aquifoliaceae). *J. Syst. Evol.* **59**, 73–82 (2021).
59. Emms, D. M. & Kelly, S. OrthoFinder: phylogenetic orthology inference for comparative genomics. *Genome Biol.* **20**, 1–14 (2019).
60. Chen, S., Zhou, Y., Chen, Y. & Gu, J. fastp: an ultra-fast all-in-one FASTQ preprocessor. *Bioinformatics* **34**, i884–i890 (2018).
61. Li, H. et al. Aligning sequence reads, clone sequences and assembly contigs with BWA-MEM. Preprint at https://arxiv.org/abs/1303.3997 (2013).
62. Danecek, P. et al. Twelve years of SAMtools and BCFtools. *GigaScience* **10**, giab008 (2021).
63. Wong, T. K. F. et al. IQ-TREE 3: phylogenomic inference software using complex evolutionary models. *Mol Biol Evol.***43**, msag117 (2026).
64. Mirarab, S. et al. ASTRAL: genome-scale coalescent-based species tree estimation. *Bioinformatics* **30**, i541–i548 (2014).
65. Zhang, C., Nielsen, R. & Mirarab, S. ASTER: a package for large-scale phylogenomic reconstructions. *Mol. Biol. Evol.* **42**, msaf172 (2025).
66. Tabatabaee, Y., Zhang, C., Warnow, T. & Mirarab, S. Phylogenomic branch length estimation using quartets. *Bioinformatics* **39**, i185–i193 (2023).
67. Demotte, P. et al. IQ2MC: a new framework to infer phylogenetic time trees using IQ-TREE 3 and MCMCTree with mixture models. Preprint at https://doi.org/10.32942/X2CD2X (2025).
68. Yang, Z. et al. PAML 4: phylogenetic analysis by maximum likelihood. *Mol. Biol. Evol.* **24**, 1586–1591 (2007).
69. Rambaut, A., Drummond, A. J., Xie, D., Baele, G. & Suchard, M. A. Posterior summarization in Bayesian phylogenetics using Tracer 1.7. *Syst. Biol.* **67**, 901–904 (2018).
70. Axelrod, D. I. The eocene copper basin flora of northeastern *Nevada*. *Univ. Calif. Publ. Geol. Sci.* **59**, 1–83 (1966).
71. Li, Y.-L. et al. The fossil record of *Berberis* (Berberidaceae) from the Palaeocene of NE China and interpretations of the evolution and phytogeography of the genus. *Rev. Palaeobot. Palynol.* **160**, 10–31 (2010).
72. Ramírez, J. L. & Cevallos-Ferriz, S. R. S. Leaves of Berberidaceae (*Berberis* and *Mahonia*) from Oligocene sediments, near Tepexi de Rodriguez, Puebla. *Rev. Palaeobot. Palynol.* **110**, 247–257 (2000).
73. Rueden, C. T. et al. ImageJ2: ImageJ for the next generation of scientific image data. *BMC Bioinform* **18**, 529, PMID 29187165 (2017).
74. Revell, L. J. phytools 2.0: an updated R ecosystem for phylogenetic comparative methods (and other things). *PeerJ.* **12**, e16505 (2024).
75. Rabosky, D. L. Automatic detection of key innovations, rate shifts, and diversity-dependence on phylogenetic trees. *PLoS ONE* **9**, e89543 (2014).
76. Mitchell, J. S. & Rabosky, D. L. Bayesian model selection with BAMM: effects of the model prior on the inferred number of diversification shifts. *Methods Ecol. Evo.* **8**, 37–46 (2017).
77. Matzke, N. J. BioGeoBEARS: BioGeography with Bayesian (and likelihood) evolutionary analysis in R scripts (version 0.2.1). https://CRAN.R-project.org/package=BioGeoBEARS (2013).

78. Ree, R. H., Moore, B. R., Webb, C. O. & Donoghue, M. J. A likelihood framework for inferring the evolution of geographic range on phylogenetic trees. *Evolution* **59**, 2299–2311 (2005).
79. Beaulieu, J. M. & O'Meara, B. C. Detecting hidden diversification shifts in models of trait-dependent speciation and extinction. *Syst. Biol.* **65**, 583–601 (2016).
80. FitzJohn, R. G. Diversitree: comparative phylogenetic analyses of diversification in R. *Methods Ecol. Evol.* **3**, 1084–1092 (2012).
81. Onstein, R. E. et al. Frugivory-related traits promote speciation of tropical palms. *Nat. Ecol. Evol.* **1**, 1903–1911 (2017).
82. Höhna et al. Bayesian phylogenetic inference using graphical models and an interactive model-specification language. *Syst. Biol.* **65**, 726–736 (2016).
83. Kong, H. et al. Phylogenomic and macroevolutionary evidence for an explosive radiation of a plant genus in the Miocene. *Syst. Biol.* **71**, 589–609 (2021).
84. Tribble, C. et al. RevGadgets: an R package for visualizing Bayesian phylogenetic analyses from RevBayes. *Methods Ecol. Evol.* **13**, 422–432 (2022).
85. Brown, J. L. & Carnaval, A. C. A tale of two niches: methods, concepts and evolution. *Front Biogeogr.* **11**, e44158 (2019).
86. Karger, D. N. et al. CHELSA-W5E5: daily 1 km meteorological forcing data for climate impact studies. *Earth Syst. Sci. Data* **15**, 2445–2464 (2023).
87. Warren, D. L., Glor, R. E. & Turelli, M. ENMTools: a toolbox for comparative studies of environmental niche models. *Ecography* **33**, 607–611 (2010).
88. Schoener, T. W. The Anolis lizards of Bimini: resource partitioning in a complex fauna. *Ecology* **49**, 704–726 (1968).
89. Phillips, S. J. & Dudík, M. Modeling of species distributions with Maxent: new extensions and a comprehensive evaluation. *Ecography* **31**, 161–175 (2008).
90. Valdes, P. et al. The BRIDGE HadCM3 family of climate models: HadCM3@Bristol v1.0. *Geosci. Model Dev.* **10**, 3715–3743 (2017).
91. Scotese, C. R. Tutorial: PALEOMAP PaleoAtlas for GPlates and the PaleoData Plotter Program. http://www.earthbyte.org/paleomap-paleoatlas-for-gplates/ (2016).
92. Foster, G. L., Royer, D. L. & Lunt, D. J. Future climate forcing potentially without precedent in the last 420 million years. *Nat. Commun.* **8**, 14845 (2017).

Acknowledgements

We are grateful to Mr. Julian Harber (UK) for his continued guidance and support of our studies on *Berberis*. We thank the curators and staff of the Field Museum of Natural History (USA), Missouri Botanical Garden (USA), Royal Botanic Garden Edinburgh (UK), Royal Botanic Gardens, Kew (UK), California Botanic Garden (USA), the Herbarium of the Kunming Institute of Botany (KIB, China), and the Herbarium of the Institute of Botany, Chinese Academy of Sciences (PE, China) for their assistance with specimen examination, taxonomic verification, and tissue sampling. We thank the Germplasm Bank of Wild Species at the Kunming Institute of Botany (China) for facilitating DNA extraction and sequencing from herbarium and historic collections. We thank Mr. Hongxi Zhang for assistance with field sampling and Mr. Ke (Jungle) Liang for assistance with leaf trait measurements. We thank Drs. Kuo-Fang Chung, Kyle Tomlinson, and Sheng-Feng Shen for their long-term support and encouragement throughout this project, and Drs. Qiuyue Zhang, Linbo Jia, Jian Huang, and Wenna Ding for their constructive comments on earlier versions of the manuscript. Computational analyses were supported by the Grainger Bioinformatics Center at the Field Museum of Natural History through the provision of bioinformatic infrastructure and computing resources.

Author contributions

C.-C.Y., R.H.R. and Y.-W.X. conceptualized and designed this study. C.-C.Y. and Y.-W.X. conducted the field work and sampling in China. C.-C.Y. collected and curated the leaf trait data. C.-C.Y. and Z.-Q.D. generated and curated the genomic data. C.-C.Y. performed phylogenomic, molecular dating, phylogenetic comparative and biogeographic analyses with guidance from Y.-W.X. and R.H.R. C.-C.Y. and S.-F.L. conducted niche divergence and modeling analyses. R.H.R. and R.E.O. provided methodological guidance and supervised the SSE analyses. Y.-W.X. supervised the project. C.-C.Y. and R.H.R. wrote the manuscript, and all authors edited and revised it.

Funding

This work is supported by National Natural Science Foundation of China (National Science Foundation of China to Y.-W. Xing)–32225005; The 14th Five-Year Plan of the Xishuangbanna Tropical Botanical Garden, Chinese Academy of Sciences (XTBG-1450101 and XTBG-1450102 to Y.-W. Xing), Yunnan Revitalization Talent Support Program-Yunling Scholar Project (XDYC-YLXZ-2023-0029 to Y.-W. Xing), the Young and Middle-aged Academic and Technical Leaders of Yunnan (No. 202305AC160051 to S.-F. Li) and the Yunnan Fundamental Research Projects (202501BC070013 to Y.-W. Xing).

Competing interests

The authors declare no competing interests.

Additional information

Supplementary information The online version contains supplementary material available at https://doi.org/10.1038/s41467-026-75790-3.

Correspondence and requests for materials should be addressed to Richard H. Ree or Yao-Wu Xing.

Peer review information *Nature Communications* thanks Jianquan Liu and Nicolai Nürk for their contribution to the peer review of this work. A peer review file is available.